Int. J. Electrochem. Sci., 12 **(2017)** 10800 – 10812, doi: 10.20964/2017.11.37

International Journal of
ELECTROCHEMICAL
SCIENCE
www.electrochemsci.org

Effect of Multifunctional $(NH_4)_2SO_4$ and Co-deposition Factors on Porous Copper Film

Chao Ma[1], Yue Kou[1], Zhishuang Song[1], Yingbo Li[1],Shengxiang Qu[1], Jie Liu[1], Xiaopeng Han[2], Yida Deng[2], Wenbin Hu[1,2] and Cheng Zhong[1,2,]*

[1]Key Laboratory of Advanced Ceramics and Machining Technology (Ministry of Education), School o f Materials Science and Engineering, Tianjin University, Tianjin 300072, China
[2]Tianjin Key Laboratory of Composite and Functional Materials, School of Materials Science and Engi neering, Tianjin University, Tianjin 300072, China
[*]E-mail: cheng.zhong@tju.edu.cn

Received: 1 August 2017 / *Accepted:* 11 September 2017 / *Published:* 12 October 2017

In this study, porous copper film was prepared by a co-deposition process, which used $(NH_4)_2SO_4$, a hydrogen source, as dynamic templates. To improve the morphology of porous copper film, sodium citrate was added into the base co-deposition solution as a chemical additive. The phase composition of co-deposited porous copper film was examined by X-ray diffractometer (XRD), while its morphology and nanostructure features were characterized by scanning electron microscopy (SEM) and transmission electron microscopy (TEM). The porous copper films with earhead-like nanodendrites were synthesized in the base deposition solution by the addition of $(NH_4)_2SO_4$ which served as an appropriate hydrogen source and suppressed both copper deposition and hydrogen bubbles coalescence. Meanwhile, the porous copper film obtained from the optimized solution containing $(NH_4)_2SO_4$ and sodium citrate displayed better morphology and structure features. The effect mechanism of $(NH_4)_2SO_4$ and sodium citrate on the morphology and nanostructure of porous copper film at a 3.0 A cm^{-2} current density was discussed. Moreover, the effects of $CuSO_4$ concentration and co-deposition current density on porous copper films were respectively investigated. The results demonstrated that the pore size and wall thickness would remarkably increase while the $CuSO_4$ concentration increased. Besides, the porous copper structure started to appear with the walls becoming denser when co-deposition current density increased.

Keywords: porous copper film; $(NH_4)_2SO_4$; sodium citrate; $CuSO_4$ concentration; current density

1. INTRODUCTION

Materials with larger specific surface areas are more conducive to mass (gas) transport and electricity conductivity, which could quicken the electrochemical reactions [1-4]. Therefore, three-dimensional porous metal materials become a hot topic for both academic research and practical

applications, such as catalysts [5], separation systems [6], fuel cells [7], batteries [8-9], sensors [10], supercapacitors [11] and electronic materials [12]. The traditional fabrication processes of porous metallic materials, such as hard template synthesis and dealloying [13-14], usually has weakness on controlling the thickness and porosity of 3D uniform porous materials. And these traditional methods inevitably use a costly and complicated post-treatment process to form a porous structure and morphology in the final phase . Therefore, a simple and fast preparation process is expected to develop the porous metallic materials.

Fortunately, the hydrogen bubble dynamic template was proposed and developed by Shin et al [15]. It is a process that metal ions deposition co-occurs with hydrogen bubbles evolution at high overpotential. During the co-deposition, the hydrogen ion (H^+) participates the reduction reaction and turns into floating hydrogen bubbles which is used as dynamic templates. Simultaneously, the metal ions deposit continuously around the hydrogen bubbles, forming a 3D porous structure on the working electrode [16]. Compared with traditional methods, the co-deposition process could prepare porous structure distributed with desirable pore size more simply and inexpensively, because the eliminating process of the complex procedure by hard template can be avoided. As we all know that there are several factors influencing the co-deposition, such as electrolyte composition, current density [17], temperature, and the additive especially. Most of popular base electroplating solution for the preparation of porous copper is made up by cupric sulfate ($CuSO_4$) and sulfuric acid (H_2SO_4). The critical function of H_2SO_4 is to improve the conductivity of aqueous solution and supply the hydrogen bubbles [18], although a few research groups have already reported that using $(NH_4)_2SO_4$ as chemical additive to control the morphology and nanostructure of porous copper is an effective method. The study of Kim et al. [19] demonstrated that NH_4^+, an additional hydrogen source under the co-deposition process doesn't show any indication of hydrogen evolution. Oppositely, it controls the total cathode reactions by means of adsorbing on the working electrode surface . Nam et al. [20] found that the prepared porous copper shows considerably advanced mechanical strength and stiffness when the addictive is only $(NH_4)_2SO_4$, because of its self-supporting influence from closely interlocked needle-like dendrites. However, the research discussing the porous copper film prepared by co-deposition with base solution containing aqueous solution of $CuSO_4$ and $(NH_4)_2SO_4$, its morphology and nanostructure and formation mechanism haven't been started so far. To the best of our knowledge, there are so many investigations on addictives applied to the preparation of porous copper film by co-deposition process [1-3,21], but the reports related to sodium citrate employed for the porous copper film preparation are limited and not detailed.

In this work, $(NH_4)_2SO_4$ was used to prepare the porous copper film to act as the hydrogen source and suppress the hydrogen bubbles coalescence during co-deposition process. Meanwhile, sodium citrate was applied to modify both the morphology and nanostructure of the porous copper film. In theory, $(NH_4)_2SO_4$ is an essential accelerator for porous copper film preparation, because stable copper ion–ammine complexes could affect the copper nucleation mechanism and growth kinetics [22]. In addition, it is reported that ammonia is an important additive to form acicular-shaped or needle-shaped particles and long strands or rod-shaped nanodendrites [23]. As demonstrated, increasing the concentration of sulfate ions could decrease hydrogen bubbles coalescence probability and contribute to increasing the number of hydrogen bubble template [16]. Thus, the porous copper

film would be obtained and its nanostructure and mechanical properties would be effected with $(NH_4)_2SO_4$ [18].

Sodium citrate has been widely served as an effective complexing agent in copper-nickel alloys production by balancing the practical reduction potentials between copper and nickel to achieve a desirable alloy [24]. And sodium citrate, serving as an inhibitor for copper deposition, would improve the morphology of porous copper film by suppressing dendrite growth [25].

Hence, the aim of this study is to adjust the $(NH_4)_2SO_4$ concentration to analyze its multifunction in the co-deposition process and to investigate the effect of sodium citrate on morphology and nanostructure of porous copper film. The effects of the $CuSO_4$ concentration and the co-deposition current density on the morphology of porous copper film were also studied respectively. At last, the porous copper film prepared from the most optimized co-deposition solutions without sulfate was be characterized and its formation mechanism was discussed.

2. EXPERIMENTAL

2.1 Reagents

The chemical reagents including $CuSO_4$, sodium citrate and $(NH_4)_2SO_4$ were AR grade in the experiments. $CuSO_4$ and $(NH_4)_2SO_4$ were purchased from Sinopharm Chemical Reagent Co., Ltd. sodium citrate purchased from Tianjin Yuanli Chemical Co., Ltd. All chemicals were used as received without further purification.

2.2 Preparation of Copper Films by Electrodeposition

The deposited nonporous copper film and the co-deposited porous copper film were prepared from electro-deposition process in Sulfate bath by IviumStat workstation using a two-electrode cell. The pure copper sheet acted as the cathode with a work area of 10 × 10 mm and the other pure copper sheet with an area of 30 × 40 mm served as the anode [2]. All solutions were made up with ultrapure water. Prior to use, pure copper sheet was washed by ethanol and the 1 M hydrochloric acid respectively, and then polished by #2000 water proof abrasive paper [26].

Firstly, a base solution for the nonporous copper deposition was made up with 0.1 M $CuSO_4$. It was stirred mechanically about 30 min before the electro-deposition in order to remove insoluble substances. Secondly, different amounts of $(NH_4)_2SO_4$ were added into the base deposition solution from 0.5 to 1.0, and 2.0 M, respectively to analyze the multifunction of $(NH_4)_2SO_4$ in the co-deposition process. And the aqueous solution consisting of 0.1 M $CuSO_4$ and 1.0 M $(NH_4)_2SO_4$ was called the base co-deposition solution for preparing porous copper film. Thirdly, the most optimized co-deposition solution involves a moderate concentration (0.3 M) of sodium citrate, a novel additive used to improve the morphology and nanostructure of porous copper film. Furthermore, a series of electrolytes with different $CuSO_4$ concentration and current densities were set to study the effect of both the copper ion concentration and the current density on the morphology and nanostructure of the

porous copper film. The co-deposition was carried out in a stationary aqueous solution. All the experiments were repeatedly performed and repeatable results were able to be obtained.

2.3 Characterizations

Bruker D8 Advanced X-ray diffractometer (XRD) with Cu Kα radiation at a scanning rate of 5° min^{-1} from 20° to 95° was applied to characterize the phase composition of the dried copper co-deposition raked out from the substrate with tweezers [27]. Scanning electron microscopy (SEM, s4800, 30 kV) was used to investigate the morphology and structure of porous copper film. The image analysis software, Nano Measurer 1.2, was employed to conduct the average pore size and wall thickness of the surface layer of each porous copper film sample [2]. Furthermore, for transmission electron microscopy (TEM, JEM-2100f, 200 kV) analysis, the dried co-deposition copper film was raked out from the substrate with tweezers, and then uniformly dispersed in ethanol by sonication [19]. The crystal structure of copper co-deposition was identified by selected area electron diffraction (SAED) analysis. In addition, the pH meter (IS126C) was used to test the pH of both the base deposition solution and the optimized co-deposition solution.

3. RESULTS and DISCUSSION

3.1 Effect of $(NH_4)_2SO_4$ on the Structure and Morphology of Porous Copper Film

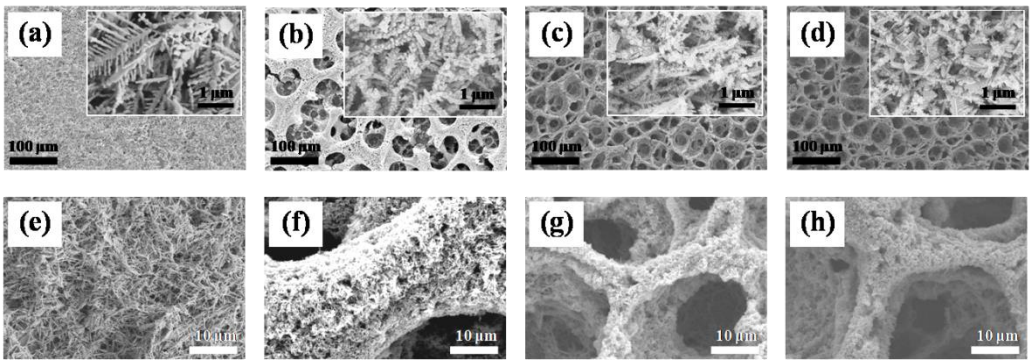

Figure 1. SEM images with different magnifications of the co-deposited porous copper films at a 3.0 A cm^{-2} cathode current density in the base solutions added with no additive (a and e), 0.5 M $(NH_4)_2SO_4$ (b and f), 1.0 M $(NH_4)_2SO_4$ (c and g), and 2.0 M $(NH_4)_2SO_4$ (d and h) for 15 s.

Fig. 1 displays the typical SEM images of the porous copper films prepared by co-deposition at 3.0 A cm^{-2} for 15 s. Images in the Fig. 1 show a porous copper structure in spite of different content of $(NH_4)_2SO_4$, except the Fig. 1a and e which shows a non-porous structure. It is worth noting that the concentration of $(NH_4)_2SO_4$ influences the morphology of the porous copper films, including compactness degree of porous wall, the average pore size and the density of pore. As exhibited in Fig.

1a and e, the copper sample formed from the base solution shows loosen but uniform morphology. It can be concluded that sufficient hydrogen source is key and necessary for the preparation of porous copper film during co-deposition process. In other words, the porous copper films shown in Fig. 1b–d and Fig. 1f–h were obtained successfully thanks to the adequate NH_4^+ ions, which plays a critical role, namely hydrogen source. When there was shortage of hydrogen ions, the co-deposition process was difficult to carry out and copper deposition occurred, because the current density (3.0 A cm^{-2}) was obviously higher than the value of that in the normal process, which was easily to form numerous nucleations at different active sites on the working electrode. And there was sufficient time for Cu nucleation to grow into dendrites. As depicted in Fig. 1b–d and Fig. 1f–h, highly porous copper structure co-deposits were prepared. Though the overall morphology and nanostructure were similar to those formed from the system of $CuSO_4$ and H_2SO_4, the pore size and wall thickness of the co-deposited porous copper film were reduced [15]. The co-deposited porous copper films exhibited that a great many of interlocking earhead-like nanodendrites with high density constituted the walls of the porous copper film. It seems that the mechanical strength of the porous structure would be improved by those earhead-like nanodendrites, because they were closely connected with each other [19].

In theory, the greatly steady copper ion–ammine complexes are easy to form in an aqueous solution containing sufficient Cu^{2+} and NH_4^+ ions. Those complexes will improve the copper ions solubility and influence both the nucleation mechanism and the growth kinetics of copper [21]. Moreover, the NH_4^+ ion is known as an important accelerator to prepare needle-shaped particles, as reported that where there are the linear complexes inducing an anisotropic crystallographic deposition growth, there are long strands or rod-shaped nanodendrites in an ammonia bath [20]. As shown in Fig. 1a and Fig. 1b, the nanostructure of porous copper film is transformed from fish-bone nanostructure to earhead-like deposit due to the addition of $(NH_4)_2SO_4$.

As shown in Fig. 1b–d and f–h, increasing concentration of $(NH_4)_2SO_4$ approximately decreases the mean pore size (from 60 μm to 30 μm) and the average wall thickness (from 20 μm to 6 μm), while the uniformity of co-deposited porous copper film is enhanced. Generally speaking, hydrogen bubbles were mainly formed by nucleation and growth on the surface of working electrode. They are supposed to gradually get away from the substrate and expand quickly because of a force to float up the bubbles and the random coalescence of neighboring bubbles [31-32]. The effect of sulfate ions on the hydrogen bubbles, demonstrated by Zhang et al. [16], is suppressing the hydrogen bubbles coalescence. Hence, increasing the concentration of $(NH_4)_2SO_4$ will decrease the probability of adjacent hydrogen bubbles coalescence, increase the number of hydrogen bubbles at dynamic template, reduce their mean distance, and eventually shorten the mean pore size [16]. In this part, with gradually adding $(NH_4)_2SO_4$, the amount of hydrogen bubbles per unit area should be increased. There is the greater chance for hydrogen bubbles coalescence and the pore size on the top layer would be larger than the former. However, this phenomenon was not observed from Fig. 1b–d and f–h, thus the $(NH_4)_2SO_4$ actually suppresses the hydrogen bubbles coalescence.

The NH_4^+ ion, acting as an additional hydrogen source, shows no indication for hydrogen evolution under the co-deposition process, but rather inhibits the total cathode reaction by means of adsorbing on the working electrode surface, reported by Kim et al. [18]. However, Fig. 1 shows a different view. The visual evidence for hydrogen bubbles generation, growth and coalescence via

reduction reaction of H^+ which roots in the hydrolysis of NH_4^+ was recognized. Thus we regarded NH_4^+ as a power source to increase porosity of copper film [33].

Moreover, when the hydrogen source, NH_4^+, is combined with sulfate ions, suppressive effect on bubbles coalescence exists in the co-deposition solution [34]. Furthermore, Adding $(NH_4)_2SO_4$ can change the nanostructure of porous copper film. In summary, it can be concluded that $(NH_4)_2SO_4$ has a multifunctional effect which could replace H_2SO_4 as an appropriate candidate and influences not only the copper deposition but also the hydrogen evolution. And the concentration of $(NH_4)_2SO_4$ added to the co-deposition solution also has inseparable connection with the pore size, the pore density and the wall thickness of the porous copper film [2, 13].

3.2 Effect of Sodium Citrate on the Morphology of Porous Copper Film

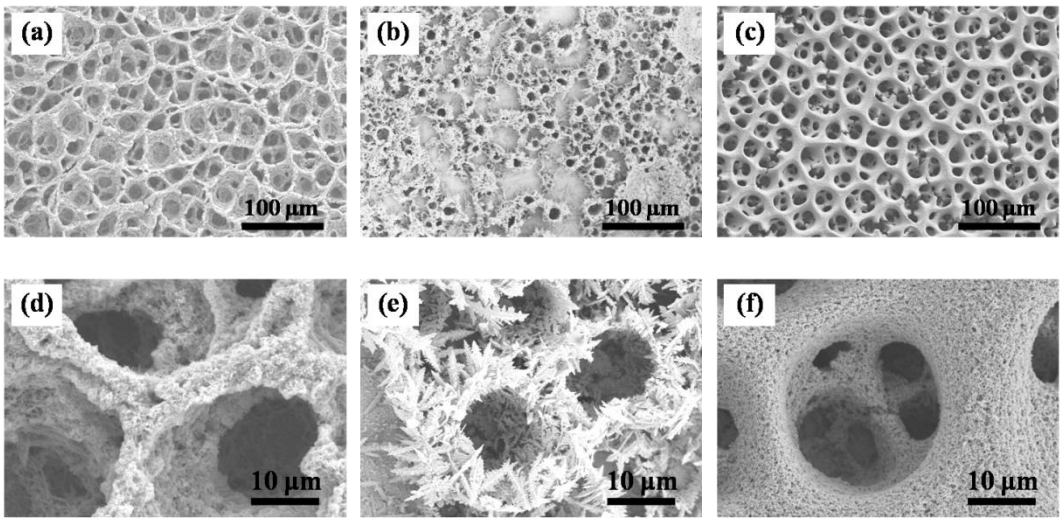

Figure 2. SEM images with different magnifications of the co-deposited porous copper films at 3.0 A cm^{-2} cathode current density in the base solution added with 1.0 M $(NH_4)_2SO_4$ (a and d) + 0.3 M sodium citrate (b and e), and 1.0 M $(NH_4)_2SO_4$ + 0.3 M sodium citrate (c and f) for 15 s.

Fig. 2 displays typical SEM images exhibiting the influence of sodium citrate on the structure and morphology of porous copper films prepared by co-deposition at 3.0 A cm^{-2} for 15 s. It is evident that both Fig. 2a and Fig. 2c show a porous structure, but Fig. 2b displays an inhomogeneous deposited copper which features a single-layer structure with a number of dendrites and pores at random. Besides, the details of porous copper film in Fig. 2a and Fig. 2c look obviously different, especially in mean pore size and the thickness and compactness degree of the wall. Compared with the porous copper film prepared from the base co-deposition solution (as shown in Fig. 2a), the deposition obtained from the optimized solution ((as shown in Fig. 2c) shows smaller mean pore size (23 μm), thicker wall (12 μm) and a higher compactness degree of the wall. The deposition formed from the $(NH_4)_2SO_4$-free solution (Fig. 2b) displays a nonporous copper structure which suggests sufficient hydrogen source is a key factor for porous copper film. In other words, only NH_4^+ would serve as the hydrogen source for porous copper film in this study. Furthermore, the walls show rougher surface and possibly stronger mechanical strength because of denser copper dendrites and finer crystal particles

(observed from the inserts in Fig. 6c and Fig.6b). The above characteristics probably prove the fact that when sodium citrate was added into the base co-deposition solution, the function of the hydrogen source NH_4^+ changes, so does that of sulfate used to suppress the hydrogen bubbles coalescence. As observed in Fig. 2c, the morphology of co-deposition sample was vastly changed by the addition of sodium citrate despite the presence of $(NH_4)_2SO_4$. The co-deposition seems to have better mechanical strength due to higher wall compactness. The porous morphology is desirable, thanks to the particular function of copper-citrate complexes. Undoubtedly, the copper-citrate complexes have been obtained [35] and sodium citrate has influenced the copper deposition mechanism [36]. As reported, the copper-citrate complexes could adsorb on the surface of working electrode to suppress the electro-deposition of Cu^{2+} ions [37]. The experiment also shows the pH influentially increases from 3.78 to 5.24 when sodium citrate is added into the base co-deposition solution. It means the hydrogen bubble evolution will be suppressed when the total quantity of hydrogen source decreases. Furthermore, the sodium citrate is used widely and popular because of its ability to refine grain and inhibit the formation of dendrites in alloy deposition. [38]. It is meaningfully concluded that sodium citrate is able to suppress the copper dendrites electro-deposition and hydrogen reduction reaction, and helps to obtain the dense walls and fine nanostructure eventually.

3.3 Effect of $CuSO_4$ Concentration on the Pore Size and Wall Thickness of the Porous Copper Film

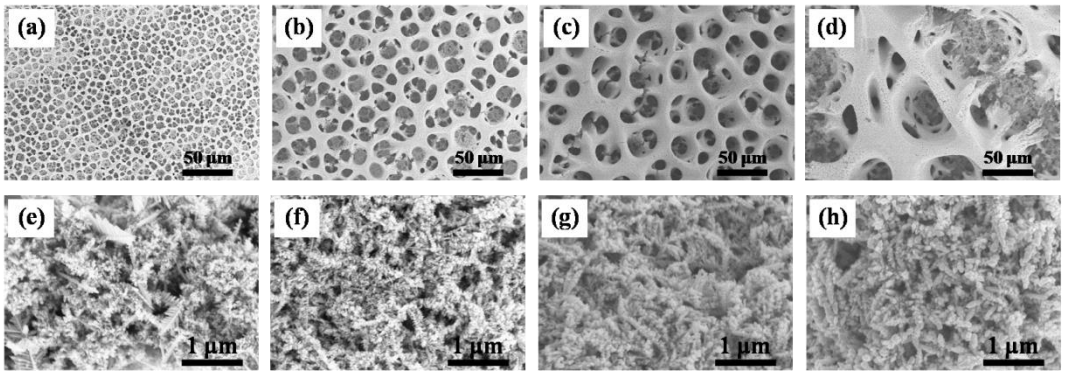

Figure 3. SEM images with different magnifications of the co-deposited porous copper films at a 3.0 A cm^{-2} cathode current density in the co-deposition solutions with 1.0 M $(NH_4)_2SO_4$, 0.3 M sodium citrate and 0.01 M $CuSO_4$ (a and e), 0.05 M $CuSO_4$ (b and f), 0.1 M $CuSO_4$ (c and g), and 0.2 M $CuSO_4$ (d and h) for 15 s.

Fig. 3 shows typical SEM images of the porous copper films obtained from the co-deposition solution with different concentrations of $CuSO_4$. The $CuSO_4$ concentration mainly has effect on the pore size and the wall thickness of the porous copper films [2]. In this study, the porous copper films were formed by the competitive deposition of copper ions and hydrogen bubbles. When current density remains constantly during the co-deposition process, the increase of copper sulfate concentration would drive up the partial current which is completely related to the reduction reaction of copper ions, but the partial current related to the hydrogen evolution would decrease. As is known to us, the decrease of the hydrogen evolution rate would affect the morphology of porous copper film. Therefore,

it is also proved that copper sulfate concentration has effect on the morphology of porous copper film. As expected, the pore size and wall thickness evidently change with the increase of $CuSO_4$ concentration. In detail, the pore size increases from 10 μm to 40 μm and the wall thickness changes from 3 μm to 10 μm while the copper ion concentration increases from 0.01 to 0.1 M.

The whole evolution process of hydrogen bubbles in co-deposition process can be divided into six steps, nucleation, growth, departure from the substrate surface, collision, coalescence, and final rupture [39]. The higher hydrogen reduction rate, the more hydrogen bubbles. It will powerfully stir the solution around the working electrode and accelerate the solution convection, which could effectively remove the hydrogen bubbles from the working electrode surface. In short, the higher hydrogen bubble evolution rate would help to form smaller hydrogen bubbles leaving from the working electrode surface. In other words, the pore size of the co-deposition porous copper film goes smaller when the concentration of Cu^{2+} ions decreases. As shown in Fig. 3, where there is the lowest concentration of Cu^{2+} ions, there is the smallest pore size of the co-deposition porous copper film. In conclusion, the most desirable porous copper film with honeycomb was obtained when Cu^{2+} ions concentration remains in a range of 0.01 to 0.1 M. Until the Cu^{2+} ions concentration reached 0.2 M, the structure of porous copper film began to gradually collapse with destroyed morphology though the nanostructure remained unchanged, which should be attributed to an excessive cathode polarization resulted from the copper electrodeposition.

3.4 Effect of Current Density on Preparation of Porous Copper Film

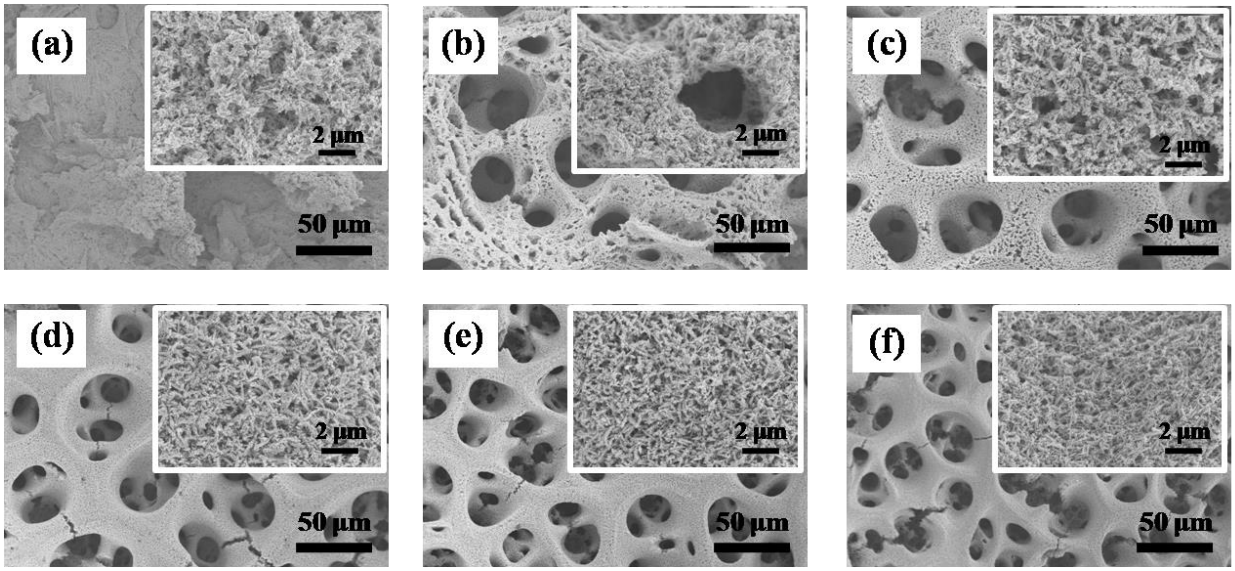

Figure 4. SEM images with different magnifications of the co-deposited porous copper films in the base co-deposition solutions of 0.1 M $CuSO_4$ + 1.0 M $(NH_4)_2SO_4$ + 0.3 M sodium citrate at a different cathode current density of 0.5 A cm^{-2} (a), 1.0 A cm^{-2} (b), 1.5 A cm^{-2} (c), 2.0 A cm^{-2} (d), 2.5 A cm^{-2} (e) and 3.0 A cm^{-2} (f) for 90 s, 45 s, 30 s, 22.5 s, 18 s, 15 s respectively.

Fig. 4 shows the evolution of morphology and structure of co-deposited porous copper films in the aqueous solution of 0.1 M $CuSO_4$, 1.0 M $(NH_4)_2SO_4$ and 0.3 M sodium citrate at diverse current

density within the range of 0.5–3.0 A cm^{-2}. As observed from the Fig. 4a, once the current density is lower than 0.5 A cm^{-2}, the porous structure is difficult to form even if the hydrogen source is sufficient. If the current density is lift up to 2.0 A cm^{-2}, interconnected porous copper structure appears on the working electrode surface and numerous apparent smaller pores in the walls obviously can be seen. Meanwhile, the dendrites show a pleasant trend to grow towards the interior of micropores which will lead to obtain denser walls and better mechanical porous structure. So, the proper increase of the current density is able to promote the formation of porous copper films. According to the existing reports, the porous copper film is mainly resulted from the co-deposition between copper deposition and hydrogen evolution [2] at a properly high overpetential. Different dynamic templates will be obtained when current density changes. For example, sizes and amounts of hydrogen bubbles are different due to the co-deposition current dominating the hydrogen evolution rate. When current density stays low, few hydrogen bubbles are produced on the substrate surface, causing interconnected porous copper film failing to form because of too much available area for copper deposition on the working electrode. In other words, the current, under a low current density, is mainly used for the growth of copper earhead-like dendrites on the working electrode surface. With the increase of current density, a large number of hydrogen bubbles formed, grown and clustered. It will control the nucleation and growth of copper ions and make copper reduction reaction only taking place at the interstices of hydrogen bubbles [40]. As observed from Fig. 4d–f, when the current density subsequently changed from 2.0 A cm^{-2} to 3.0 A cm^{-2}, the porous morphology didn't change too much. The surface pore size, the wall thickness and the quantity of the wall crack were all similar while all co-depositions possessed porous structure.

In conclusion, with the increase of current density in a particular range, the pore size clearly becomes smaller and the wall becomes denser, which should be attributed to the hydrogen reduction rate accelerated by the increase of the current density, finally leading to the generation of smaller bubbles and copper growth towards the interior of the wall [40].

3.5 Preparation and Characterization of Most Preferred Porous Copper Film

Fig. 5 shows several typical SEM images of the co-deposited porous copper film at the optimized condition which includes an aqueous solution of 0.1 M $CuSO_4$, 1.0 M $(NH_4)_2SO_4$ and 0.3 M sodium citrate with cathode current density of 3.0 A cm^{-2} and 15 s deposition time. It is easy to conclude from Fig. 5a that the co-deposited copper film possesses a 3D interconnected open porous structure and uniform pore size in the surface. Both Fig. 5b and Fig. 5c display the walls are composed of highly dense and unordered dendrites in every direction, which build the uniform porous structure with a self-supported capacity. The characteristic pores size and wall thickness in the co-deposited porous copper film is around 23 μm and 10 μm respectively (Fig. 5b), because co-deposition process including a competitive behavior of both metal ions deposition and the hydrogen evolution occurs in a high overpotential and a proper co-deposition electrolyte. This process usually contains two reactions as shown by the equations below [20]:

$$2NH_4^+ + 2e^- \rightarrow 2NH_3 + H_2 \quad (1)$$

$$Cu^{2+} + 2e^- \rightarrow Cu \quad (2)$$

Actually, if the hydrogen bubble has already existed, the availability of copper ions and co-deposition would not happen.

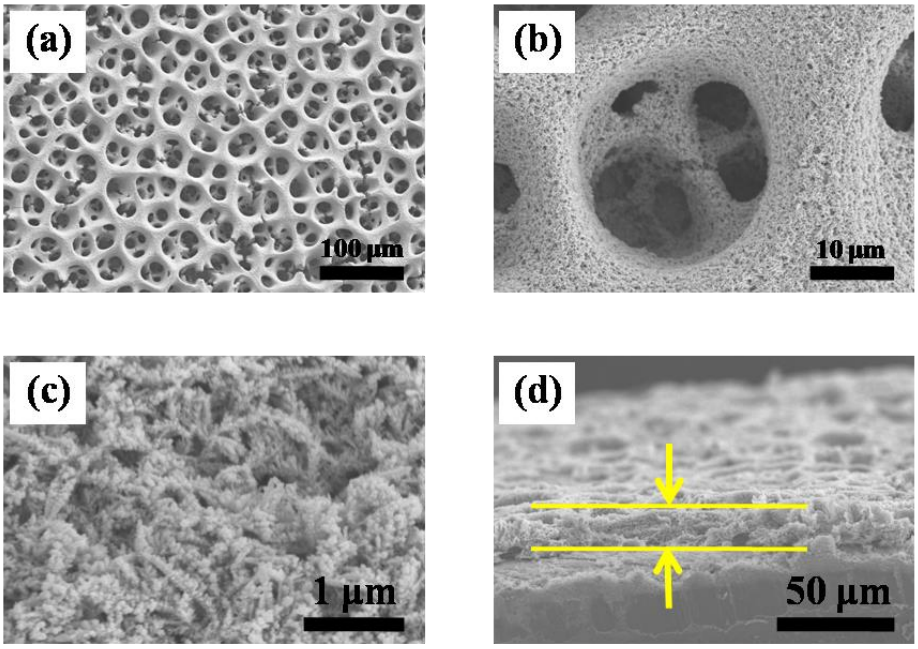

Figure 5. Top-view and side-view SEM images with different magnifications of the co-deposited porous copper film at a 3.0 A cm^{-2} cathode current density in an aqueous solution of 0.1 M $CuSO_4$ + 1.0 M $(NH_4)_2SO_4$ + 0.3 M sodium citrate for 15 s.

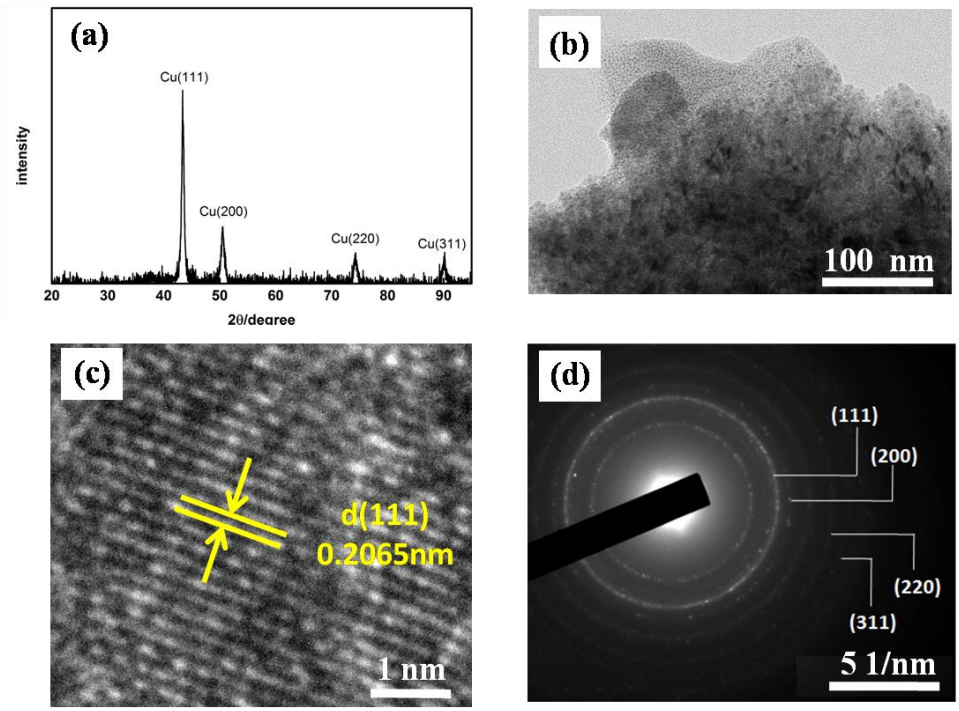

Figure 6. XRD pattern (a), TEM image (b), high-resolution TEM (HRTEM) (c) and corresponding selected area diffraction (SAED) pattern (d) of the co-deposited porous copper film at a 3.0 A cm^{-2} cathode current density in a base co-deposition solution of 0.1 M $CuSO_4$ + 1.0 M $(NH_4)_2SO_4$ + 0.3 M sodium citrate for 15 s.

It is proved by the porous copper films that the copper growth at the place of hydrogen bubble has been restrained, which only happens around the hydrogen bubbles. Therefore, the hydrogen bubbles at different sites on the working electrode surface act as dynamic templates to fabricate the porous copper film during the co-deposition process.

As shown in Fig. 5a and Fig. 5b, the pore size on surface is larger than that on substrate, which regularly enlarges with the increase of the distance from the substrate. In addition, as exhibited in Fig. 5d, the sectional SEM image of the porous copper film displays the thickness of film goes to 16 μm. As reported by Ying et al. [2], the hydrogen bubbles acting as dynamic templates at the surface layer of porous copper film co-deposition usually has close connect with the other hydrogen bubbles at near layers. The growth and coalescence of hydrogen bubbles create the ideal porous copper film with extremely high surface area suiting for rapid transport of electroactive gas/liquid [13]. It must be noted that the traditional 3D porous material has the uniform pore size, but its performance in the application of rapid electrochemical reactions is unsatisfactory. The reason is the small pores at the top surface usually restrict the transport of active species into the inner of the porous structure, lowering the utilization of all the surface area [28-30].

In this study, the co-deposited porous copper film with mechanically self-supported structure is able to maintain integrity after washing by deionized water, subsequent drying treatment and characterization.

Fig. 6 represents the typical XRD pattern, the TEM image, the high-resolution TEM (HRTEM) and corresponding selected area diffraction (SAED) pattern of the co-deposited porous copper film. As shown in Fig. 6a, the features of the face-centered cubic copper crystal structure are distinctly indicated by the orientations along the Cu(111), Cu(200), and Cu(220) direction. And apparent phenomenon that the peaks of copper oxide were not detected from the XRD pattern, that is to say, the peaks of copper oxide were very weak. Obviously, there is one key reason which the numerous protons in the co-deposition solution not only suppress the formation of oxide copper but also accelerate the conversion of copper ions to Cu atoms during the co-deposition. As depicted in Fig. 6b, the co-deposited copper film with an earhead-like type and uniformly fine particles reflects the SEM result in Fig. 5c [19]. Moreover, as shown in Fig. 6c, the measured lattice spacing of 0.21 nm are indexed to the (111) plane of copper which further confirms the XRD analysis. The SAED pattern of the co-deposited copper displays a relatively clear ring-like pattern and a high consistency with the XRD analysis, and the main reason is a large number of fine primary copper crystals prepared as exhibited in Fig. 6b during the co-deposition process.

4. CONCLUSIONS

The porous copper films with a desirable structure and improved morphology features were successfully prepared by a co-deposition process with hydrogen source of $(NH_4)_2SO_4$ and additive of sodium citrate into the electrolytic solution. The porous copper film formed when the alone participation of $(NH_4)_2SO_4$ in the base deposition solution. In addition, the porous copper film obtained from the co-deposition solution added with both $(NH_4)_2SO_4$ and sodium citrate possessed better

characteristic morphology than that prepared from the solution with only $(NH_4)_2SO_4$ added. Besides, the effects of $(NH_4)_2SO_4$ and sodium citrate on porous copper film co-deposition at properly high current density (3.0 A cm^{-2}) were analyzed respectively. In order to study the effect of $(NH_4)_2SO_4$ on the co-deposition process, different amounts of $(NH_4)_2SO_4$ were added into the base copper deposition solution, which showed the multifunction of $(NH_4)_2SO_4$, supplying the H^+ for co-deposition, suppressing the hydrogen bubbles coalescence and fabricating self-supporting porous structure. Additionally, sodium citrate could decrease the hydrogen bubbles evolution rate, inhibit the dendritic growth and reduce the total reduction rate, because it has strong ability to unite with H^+ and Cu^{2+} respectively.

Both Cu^{2+} concentration and current density have a significant influence on the morphology and structure of the porous copper films. The pore size and wall thickness would be markedly increased by increasing the Cu^{2+} concentration. While the current density is lower than 0.5 A cm^{-2}, a porous copper film structure can hardly be prepared by co-deposition. But interconnected porous copper film with denser walls can be prepared if the current density is continuously increased from 1.0 A cm^{-2} to 2.0 A cm^{-2}, and the features remain stable and unchanged when the current density goes up from 2.0 A cm^{-2} to 3.0 A cm^{-2}.

ACKNOWLEDGMENTS

This work was supported by the National Key Research and Development Program (No. 2016YFB0700205), National Natural Science Foundation of China (No. 51571151), National Natural Science Foundation of China and Guangdong Province (No. U1601216), and Tianjin Natural Science Foundation (No. 16JCYBJC17600).

References

1. H.C. Shin, M. Liu, *Chem. Mater*., 16 (2004) 5460
2. Y. Li, W.Z. Jia, Y.Y. Song, X.H. Xia, *Chem. Mater*., 19 (2007) 5758
3. X. Chen, B. Liu, C. Zhong, Z. Liu, J. Liu, L. Ma, Y. Deng, X. Han, T. Wu, W. Hu, J. Lu, *Adv. Energy Mater*., doi: 10.1002/aenm.201700779 (2017)
4. W. Liu, S. Zhang, N. Li, S. An, J. Zheng, *Int. J. Electrochem. Sci*., 7 (2012) 9707
5. X. Han, X. Wu, C. Zhong, Y. Deng, N. Zhao, W. Hu, *Nano Energy*, 31 (2017) 541
6. K. Kusakabe, T. Kuroda, A. Murata, S. Morooka, *Ind. Eng. Chem.Res*., 36 (1997) 649
7. Y. Liu, S. Zha, M. Liu, *Adv. Mater*., 16 (2004) 256
8. Wróbel, A. Czerwinski, *Int. J. Electrochem*. Sci., 11 (2016) 8927
9. S. Qu, Z. Song, J. Liu, Y. Li, Y. Kou, C. Ma, X. Han, Y. Deng, N. Zhao, W. Hu, C. Zhong, *Nano Energy*, 39 (2017) 101
10. J.H. Holtz, J.S.W. Holtz, C.H. Munro, S.A. Asher, *Anal. Chem*., 70 (1998) 780
11. F. Jiang, T. Zhou, S. Tan, Y. Zhu, Y. Liu, D. Yuan, *Int. J. Electrochem. Sci*., 4 (2009) 1541
12. O. Concha, I. Castañeda, R. Guardian, A. Marban, D. Mayorga, K. Cuentas, J. Uruchurtu, M. Rincon, C. Menchaca-Campos, *Int. J. Electrochem. Sci*., 10 (2015) 6175
13. B.J. Plowman, L.A. Jones, S.K. Bhargava, *Chem. Commun*., 51 (2015) 4331
14. W. Liu, S. Zhang, N. Li, J. Zheng, S. An, Y. Xing, *Int. J. Electrochem. Sci*., 7 (2012) 6365
15. H.C. Shin, J. Dong, M. Liu, *Adv. Mater*., 15 (2003) 1610
16. W. Zhang, C. Ding, A. Wang, Y. Zeng, *J. Electrochem. Soc*., 162 (2015) D365
17. J. Niu, X. Liu, K. Xia, L. Xu, Y. Xu, X. Fang, W. Lu, *Int. J. Electrochem. Sci*., 10 (2015) 7331

18. N.D. Nikolić, G. Branković, M.G. Pavlović, K.I. Popov, *J. Electroanal. Chem*., 621 (2008) 13
19. J.H. Kim, R.H. Kim, H.S. Kwon, *Electrochem. Commun*., 10 (2008) 1148
20. D. Nam, R. Kim, D. Han, J. Kim, H. Kwon, *Electrochim. Acta*, 56 (2011) 9397
21. H. Wang, N. Wang, T. Hang, M. Li, *Appl. Surf. Sci*., 372 (2016)7
22. C. Nila, I. González, *J. Electroanal. Chem*., 401 (1996) 171
23. L. Durand-Keklikian, E. Matijević, *Colloid Polym. Sci*. , 268 (1990) 1151
24. Y. Gu, J. Liu, S. Qu, Y. Deng, X. Han, W. Hu, C. Zhong, *J. Alloys Compd.*, 690 (2017) 228
25. M.J. Kim, S. Choe, H.C. Kim, S.K. Cho, S.K. Kim, J.J. Kim, *J. Electrochem. Soc*., 162 (2015) D354
26. N.D. Nikolić, G. Branković, *Electrochem. Commun*., 12 (2010) 740
27. J. Liu, X. Fan, X. Liu, Z. Song, Y. Deng, X. Han, W. Hu, C. Zhong, *ACS Appl. Mater. Inter.*, 9 (2017) 18856
28. H.C. Shin, J. Dong, M. Liu, *Adv. Mater*., 15 (2003) 1610
29. H.C. Shin, J. Dong, M. Liu, *Adv. Mater*., 16 (2004) 237
30. H.C. Shin, M. Liu, *Adv. Funct. Mater*., 15 (2005) 582
31. P.K. Weissenborn, R.J. Pugh, Langmuir, 11 (1995) 1422
32. J. Jiao, Y. He, K. Yasui, S.E. Kentish, M. Ashokkumar, R. Manasseh, J. Lee, *Ultrason. Sonochem*., 22 (2015) 70
33. C.A. Marozzi, A.C. Chialvo, *Electrochim. Acta*, 45 (2000) 2111
34. V.S.J. Craig, B.W. Ninham, R.M. Pashley, *J. Phys. Chem*., 97 (1993) 10192
35. S. Rode, C. Henninot, C. Vallières, M. Matlosz, *J. Electrochem. Soc*., 151 (2004) C405
36. E. Chassaing, K. Vu Quang, R. Wiart, *J. Appl. Electrochem*., 16 (1986) 591
37. F.I. Lizama-Tzec, L. Canché-Canul, G. Oskam, *Electrochim. Acta*, 56 (2011) 9391
38. F.I. Lizama Tzec, G. Oskam, *ECS Transactions*, 25 (2010) 195
39. Y.H. Zhao, T. Masuoka, T. Tsuruta, *Int. J. Heat Mass Transfer*, 45 (2002) 3189
40. G.A. Lange, S. Eugénio, R.G. Duarte, T.M. Silva, M.J. Carmezim, M.F. Montemor, *J. Electroanal. Chem.*, 737 (2015) 85